



Kinetics of the selective oxidation of the lignan hydroxymatairesinol to oxomatairesinol over Au/Al₂O₃ catalysts



Olga A. Simakova ^{a,b}, Elena V. Murzina ^a, Johan Wärnå ^a, Dmitry Yu. Murzin ^{a,*}

^a Laboratory of Industrial Chemistry and Reaction Engineering, Process Chemistry Centre, Åbo Akademi University, FI-20500 Åbo/Turku, Finland

^b Graduate School of Chemical Engineering, Åbo Akademi University, FI-20500 Åbo/Turku, Finland

ARTICLE INFO

Article history:

Received 4 July 2013

Received in revised form 8 August 2013

Accepted 11 September 2013

Available online 19 September 2013

Keywords:

Hydroxymatairesinol

Lignans

Gold

Oxidation

Kinetics

ABSTRACT

Lignan hydroxymatairesinol (HMR) extracted from Norway spruce knots was oxidized to the lignan oxomatairesinol (oxoMAT) in a semi-batch glass reactor under the atmospheric pressure in the presence of oxygen (5–49 vol.% in nitrogen) over 2 wt.% Au/Al₂O₃ catalyst, using propan-2-ol–water mixture as a solvent. The following kinetic parameters were determined: adsorption constants, rate constants, reaction order for reagents, and energy of activation. Through the parameter estimation the experimental data were fitted to the advanced kinetic model demonstrating a good correlation between the model and experiments.

© 2013 Elsevier B.V. All rights reserved.

1. Introduction

Lignans are important extractives, which can be found in different parts of the tree, roots, leaves, flowers, seeds and fruits. Thus, lignan hydroxymatairesinol (HMR) can be found in the large amounts from the Norway spruce (*Picea abies*) knots. Knots being undesired for pulping industry should be removed before pulping, while valuable lignans presented in this waste from pulping industry are of the great interest due to their anticarcinogenic and antioxidative properties. Since HMR is the most abundant lignan (65–85% of the lignans [1]), it is a suitable starting material for the synthesis of other essential lignans.

A new approach for the selective oxidative dehydrogenation of HMR over heterogeneous gold catalysts resulting in the formation of the lignan oxomatairesinol (oxoMAT) was previously shown [2]. The latter substance could be used as an active component for pharmaceutical and cosmetic products, as well as a color-keeping agent for textile due to its antioxidative [3] and UV-light protection properties [4].

The reaction of HMR selective oxidation to oxoMAT is in fact selective oxidation of secondary alcohols into corresponding ketones over gold catalysts, described in many papers [5–9]. However, the reaction kinetics is challenging to investigate

as HMR is a mixture of two diastereomers: (7R,8R,8'R)-(-)-7-allo-hydroxymatairesinol (HMR 1) and (7S,8R,8'R)-(-)-7-allo-hydroxymatairesinol (HMR 2), which can undergo both reactions: oxidation to oxoMAT and isomerization to each other (see Scheme 1).

In the present paper we have studied the reaction kinetics of biomass-derived lignan HMR selective oxidation to another lignan oxoMAT over gold catalysts. Pure HMR isomers at different concentration and their mixture were utilized as a substrate; moreover, oxygen partial pressure was varied. The results were fitted to the advanced model.

2. Experimental

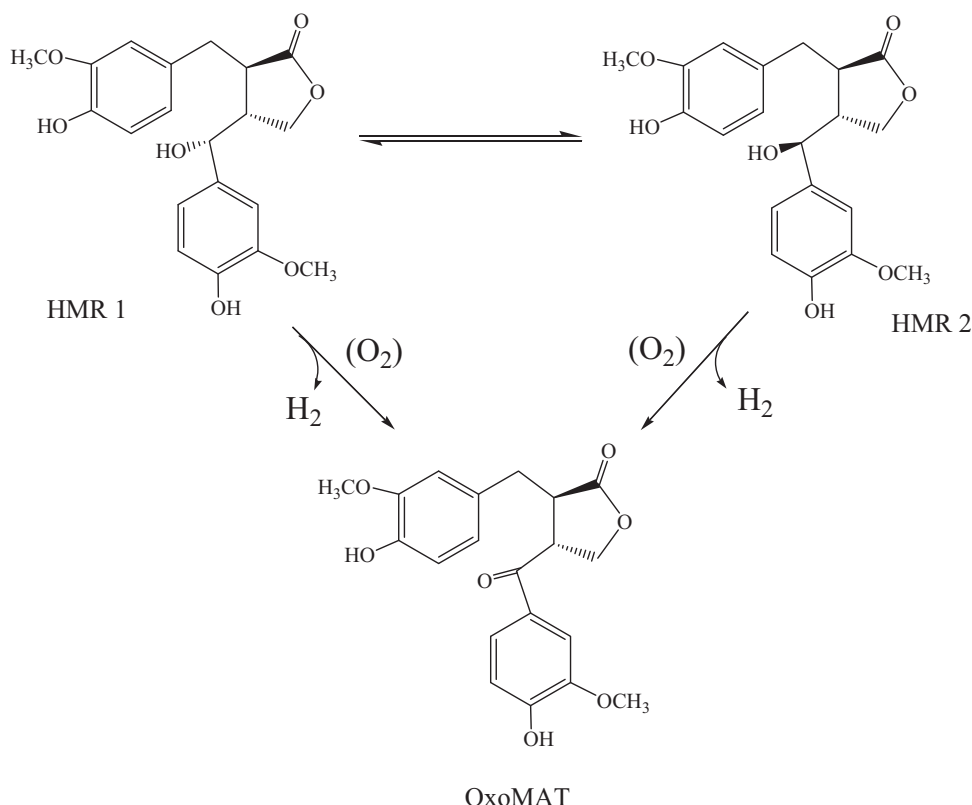
2.1. Catalyst preparation and characterization

The gold catalyst was prepared by applying a direct ion exchange method (DIE), as described elsewhere [2,10]. Alumina support (UOP, A-201, $S_{BET} = 200 \text{ m}^2/\text{g}$) was mixed with HAuCl₄ (HAuCl₄ 99.9% ABCR, Darmstadt) aqueous solution ($5 \times 10^{-4} \text{ M}$) in the amount corresponding to the final metal loading 2 wt.%. The suspension was kept under vigorous stirring for 1 h at 70 °C, than washed with ammonium hydroxide (4 M) during 1 h. The obtained powder was dried over night at 80 °C in air and after that calcined at 300 °C.

Prepared Au/Al₂O₃ catalyst was characterized by several techniques as TEM, XRD, XPS, ICP-OES. The details of applied methods

* Corresponding author. Tel.: +358 22154985.

E-mail address: dmurzin@abo.fi (D.Yu. Murzin).



Scheme 1. The reaction pathway of HMR oxidation.

and their results are given before in [2]. The most pertinent results are presented below.

2.2. Selective oxidation of hydroxymatairesinol

Hydroxymatairesinol was extracted from ground Norway spruce knots according to the procedure described in [11] as a mixture of two diastereomers of HMR: (7R,8R,8'R)-(-)-7-allo-hydroxymatairesinol (HMR 1) and (7S,8R,8'R)-(-)-7-allo-hydroxymatairesinol (HMR 2). The ratio between HMR 2 and HMR 1 in the mixture denoted further as HMR was 2 mol/mol. The purity of HMR was determined by GC to be 95%, while the main contaminant was the lignans α -conidendrin and α -conidendric acid (see Scheme 2). To utilize isolated isomers (HMR 1 and HMR 2), each one was separated from the mixture by flash chromatography. The purity of obtained lignans was 92% for HMR 1 and 85% for HMR 2.

In a typical experiment, the reaction was carried out under atmospheric pressure in a stirred 200 ml glass reactor, equipped with a heating jacket (using silicon oil as the heat transfer medium), a re-flux condenser (cooling medium set at -20°C), oil lock, pitched-blade turbine and stirring baffles. Catalyst (2 wt.% Au/ Al_2O_3 , grain size of 45–63 μm) was put into reactor. The catalysts were pre-activated in situ by heating under hydrogen (AGA, 99.999%) flow (100 ml/min) until 120°C , thereafter the reactor was cooled down to the reaction temperature under nitrogen (AGA, 99.999%) flow (100 ml/min). The reactant solution (100 ml) with HMR dissolved in 2 vol.% propan-2-ol (Sigma-Aldrich, 99.8%) was poured into the reactor. Utilizing of this mixture as a solvent allows reaching the highest activity and selectivity of gold catalysts. More details were given in [2]. The gas flow was changed to oxygen (AGA, 99.999%)-nitrogen mixture. The reaction mixture was stirred at 1000 rpm to avoid external mass transfer limitations and the experiments were performed in the kinetic regime. The reaction time set

to zero, when the stirring was started, and the first sample was withdrawn.

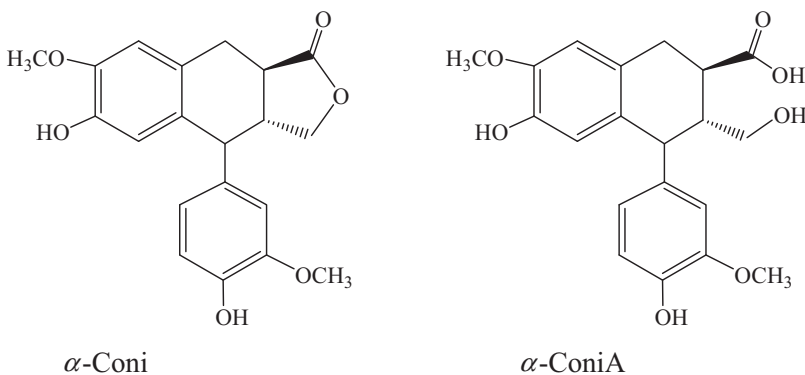
2.3. Product analysis

Samples were taken from the reactor at different time intervals and analyzed by gas chromatography (GC) using a HP-1 column (length 25 m, inner diameter 0.20 mm, film thickness 0.11 μm) and a flame ionization detector (FID) operating at 300°C . Samples, taken in the amount corresponding to the concentration of 1 mg/ml, were mixed with internal standard, which was betulinol (0.02 mg/ml) and C21:0 fatty acid (0.02 mg/ml) dissolved in methyl *tert*-butyl (MTBE, $\text{C}_5\text{H}_{12}\text{O}$). Prior to analysis, samples were silylated by N,O-bis(trimethylsilyl)trifluoroacetamide (BSTFA, 98%, Fluka). More details of the analysis procedure were given in previously published work [2].

2.4. Kinetic study

In order to study the reaction kinetics, the reaction was performed using varied concentrations of each reagent (HMR 1 and HMR 2) at the constant concentrations of reactants. Thus, to obtain the dependence of the reaction rate on HMR concentration isolated isomers were oxidized under the flow containing 24 vol.% oxygen in nitrogen, at 70°C , over 250 mg of 2 wt.% Au/ Al_2O_3 . The initial concentration of HMR 1 and HMR 2 was varied in the range: 0.006–0.049 M.

Oxygen influence was investigated by oxidizing each isomer, HMR 1 and HMR 2, at different oxygen partial pressure: 5.5–49 vol.% in nitrogen flow. The reaction conditions were kept the same for every experiment, e.g. the substrate initial concentration was ca.: 0.024 M of HMR 1 and 0.017 M of HMR 2; temperature was 70°C ; the amount of 2 wt.% Au/ Al_2O_3 was 250 mg.



Scheme 2. Structure of lignan α -conidendrin (α -Coni) and α -conidendric acid (α -ConiA).

HMR oxidation (solution concentration of 0.027 M) was performed at 70 °C with different catalyst loadings (50–800 mg) to determine the effect of the catalyst amount on the reaction rate. In all experiments 2 wt.% Au/Al₂O₃ (grain size of 45–63 μ m) was utilized.

All experiments for determination of activation energy were carried out over 200 mg of 2 wt.% Au/Al₂O₃ in the temperature range: 30–90 °C. Synthesis of oxoMAT was performed using HMR as a starting material at initial concentration of 0.027 M under synthetic air and nitrogen flow. The activation energy of isolated HMR 2 oxidation was also studied under synthetic air flow at initial concentration of 0.024 M.

2.5. Kinetic modeling

The reaction pathway of HMR oxidative dehydrogenation was described according to the Scheme 3, where oxoMAT is formed due to oxidation of both isomers HMR.

The proposed kinetic model and the equations of the batch reactor were linked to the MODEST software [12], the code was compiled and used for the parameter estimation of the data obtained in the experimental work. The rate constants, adsorption coefficients and the activation energies included in the

kinetic model were estimated from the laboratory experiments by non-linear regression with the Levenberg–Marquardt method. The reactor mass balances were solved as a subtask to the parameter estimation with the backward difference method. The parameter estimation routine minimizes the objective function, the sum of square error (Q) which is defined as

$$Q = \sum_t \sum_i (c_{i,t,\text{exp}} - c_{i,t,\text{model}})^2 w_{i,t} \quad (1)$$

where c_{exp} is the component concentration obtained from experiments and c_{est} is the component concentration predicted by the model, w is the weight factor for the experimental point. The weight factor was set to 1 for all experimental points.

The parameter estimation was performed by applying the estimation procedure directly to the data. For the parameter estimation procedure the experiments were separated in two groups. One group with experiments started with either pure HMR 1 or pure HMR 2. In the other group, the experiments were performed with a mixture of HMR 1 and HMR 2. For the second group also the activation energies could be estimated since experiments were done at different temperatures.

The mass balance for a liquid-phase component (i) in a batch reactor was written as:

$$\frac{dc_i}{dt} = \rho_B r_i \quad (2)$$

where r_i is the reaction rate and ρ_B is the catalyst bulk density ($\rho_B = m_{\text{cat}}/V$, where m_{cat} is mass of the catalyst, V is the volume of liquid phase in the reactor). The mass balance Eq. (2) is valid in the kinetic regime, i.e. in the absence of mass transfer limitations.

Kinetic model was based on the following equations:

$$z = \frac{1}{T} - \frac{1}{T_{\text{mean}}} \quad (3)$$

$$k_4 = A_4 \times \exp\left(\frac{-E_{a4}}{Rz}\right) \quad (4)$$

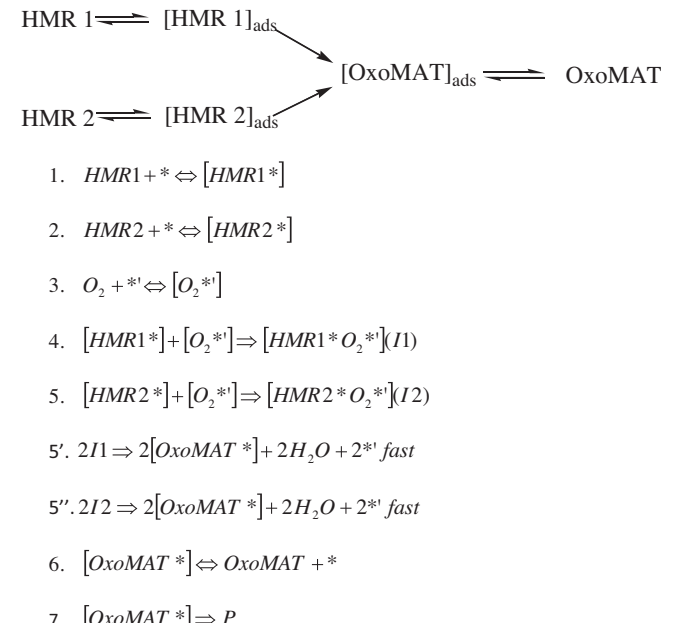
$$k_5 = A_5 \times \exp\left(\frac{-E_{a5}}{Rz}\right) \quad (5)$$

$$k_7 = A_7 \times \exp\left(\frac{-E_{a7}}{Rz}\right) \quad (6)$$

$$D = 1 + K_1 \times C_1 + K_2 \times C_2 + K_6^{-1} \times C_3 \quad (7)$$

$$a = 1 - \frac{C_p}{C_{p,\text{max}}} \quad (8)$$

$$r_4 = k_4 \times C_1 \times \frac{a}{D} \quad (9)$$



Scheme 3. (a) Reaction pathway and (b) reaction steps of HMR selective aerobic oxidation to oxoMAT over Au catalysts.

$$r_5 = k_5 \times C_2 \times \frac{a}{D} \quad (10)$$

$$r_7 = k_7 \times \frac{C_3}{D} \quad (11)$$

where T_{mean} is 70 °C, R is the molar gas constant equals to 8.314 J/K mol, A_i is the pre-exponential factor, C_1 is the concentration of isomer HMR 1, C_2 is the concentration of isomer HMR 2, C_3 is the concentration of oxoMAT, C_p is the concentration of organic compounds deposited on the catalyst surface (P), $C_{p\max}$ is the maximum concentration of organic compounds deposited on the catalyst surface, a is the activity function, r_4 and r_5 are the reaction rates of oxidation steps, r_7 is the reaction rate for formation of deposits P , k_4 , k_5 and k_7 are the corresponding lumped reaction rates constants, which include also adsorption coefficients of organic reactants and an oxygen dependent function, K_1 , K_2 , K_6 are adsorption constants. Numbering of rate constants and adsorption coefficients corresponds to the steps in **Scheme 3**.

Eq. (7) does not include explicitly adsorption of water, 2-propanol and acetone, which is a product of the 2-propanol oxidative dehydrogenation. While influence of water on kinetics can be neglected, an impact of 2-propanol and acetone cannot be ruled out. Involvement of them in the reaction mechanism was considered through the activity function, which is a lumped function and takes into account activity decline as the reaction proceeds due to deposition of coke and strong adsorption of other organic species including acetone.

Numerical data fitting clearly showed that in order to explain the experimental observations it was important to include the deactivation function, while introduction of the product inhibition was not sufficient.

The involvement of oxygen should be explained based on the zero order kinetics with respect to it, as will be described below. In order to account for such kinetic behavior oxygen is assumed to adsorb on the sites different to the ones where HMR can be adsorbed. Noncompetitive nature of adsorption along with an assumption of complete coverage of the sites for oxygen adsorption leads eventually to the zero order kinetics.

Once complexes of HMR with molecular adsorbed oxygen are formed (steps 4 and 5 in **Scheme 3**) they are further transformed to the product (steps 5' and 5'' in the same scheme). Mechanistic details of oxygen assisted dehydrogenation of HMR were recently addressed at the DFT level using the hybrid Becke's three parameters exchange correlation functional B3LYP albeit for a simple Au₂₈ cluster [13].

It should be noted here that in **Scheme 3** isomerization between HMR 1 and HMR 2 was not included, although in principle it can happen even on the surface of the support [2]. In the initial stage of kinetic modeling isomerization between HMR 1 and HMR 2

was considered in the model. Preliminary parameter estimation demonstrated, however, that the isomerization step can be in fact neglected. This is in line with the experimental data reported below showing that the consumption rate of HMR 1 was much lower than for HMR 2, which implies that the former is not transformed to a significant extent. Similar results on the absence of isomerization between HMR 1 and HMR 2 were reported in [14] for a large set of catalysts: Au ion-exchanged on Y-zeolites promoted by Cu, Ni, Fe; Au and Au-Pd supported via deposition-precipitation with urea-DPU on metal oxides (magnesia, alumina, ceria, zirconia, and lanthanum oxide); and Au on alumina, and alumina-ceria-zirconia mixed oxides prepared by the sol-gel method. The catalytic activity was correlated with the Lewis Acidity of the support and it was proposed that HMR could be adsorbed on Al-OH or Al³⁺ surface groups by oxygen bonded with αH, while αH and βH elimination is occurring on the gold particles surface.

The kinetics of HMR oxidative dehydrogenation was described with the batch reactor model with the following mass balances for each component:

$$\frac{dC_1}{dt} = -r_4 \times \frac{m_{cat}}{V} \quad (12)$$

$$\frac{dC_2}{dt} = -r_5 \times \frac{m_{cat}}{V} \quad (13)$$

$$\frac{dC_3}{dt} = (r_4 + r_5) \times \frac{m_{cat}}{V} \quad (14)$$

$$\frac{dC_p}{dt} = r_7 \times \frac{m_{cat}}{V} \quad (15)$$

3. Results and discussion

3.1. Experimental results

3.1.1. The isolated isomers HMR 1 and HMR 2 selective oxidation

For kinetic evaluation besides experimental data generated in the present work also some previously published data [2] were used. **Fig. 1** (slightly modified from [2]) presents reaction profiles for oxidative dehydrogenation of HMR 1 and HMR 2. The initial reaction rate of HMR 1 oxidation is roughly two times lower, than HMR 2 (**Fig. 1**). The reasons for different reactivity were discussed in [2] and were attributed to the different potential energy of the intermediates formed from each isomer, as well as steric hindrance.

According to the concentration profiles (**Fig. 2**), the reaction kinetics clearly shows non-zero order with respect to the substrate HMR 1 and HMR 2.

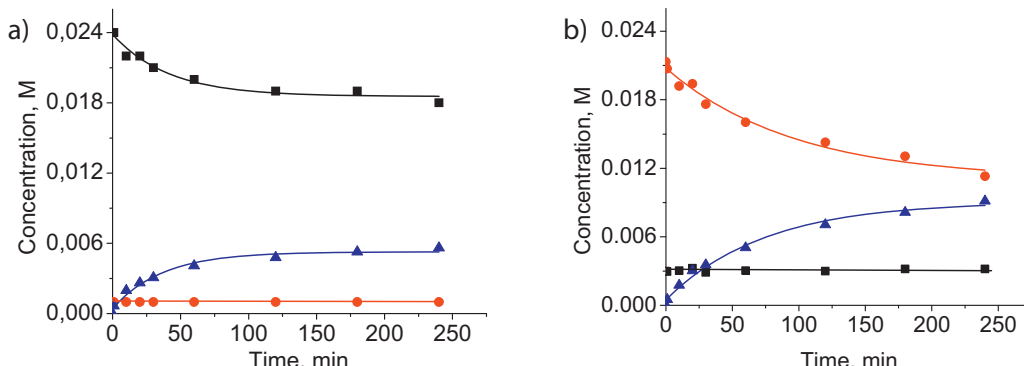


Fig. 1. Reaction profile of the selective oxidation over 250 mg of 2 wt.% Au/Al₂O₃ catalyst at 70 °C, under 24% oxygen in nitrogen flow of the isolated isomer: (a) HMR 1 initial concentration is 0.024 M, (b) HMR 2 initial concentration is 0.021 M, where (■) is HMR 1; (▲) is oxoMAT; (●) is HMR 2.

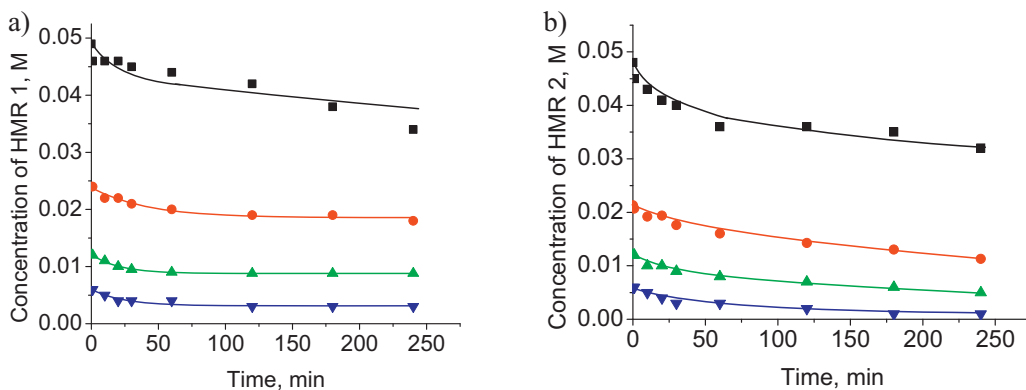


Fig. 2. Selective oxidation over 250 mg of 2 wt.% Au/Al₂O₃ catalyst at 70 °C, under 24% oxygen in nitrogen flow of the isolated isomer: (a) HMR 1 and (b) HMR 2 at different initial concentration of isomers.

Linearization of kinetic data in the logarithmic coordinates gave the apparent reaction orders of 0.42 ± 0.05 and 0.29 ± 0.07 for HMR 1 and HMR 2 isomers, respectively (Fig. 3).

The possible explanation for these results could be retardation of the reaction rate by adsorption of the product as well as substrate impurities on the catalyst active sites as elaborated in [15]. Thus, in case of HMR 1 the reaction rate significantly decreased at already 60 min, while the same happened in HMR 2 oxidation at 180 min. Previously studied kinetics of alcohols oxidation gives first-order reaction in the case of gas-phase ethanol [16,17] and methanol [18] oxidation. It is important to note, that although HMR 1 and HMR 2 can be isomerized to each other, the selectivity to oxoMAT was 100% during the reactions.

Additional complication in evaluation of the reaction order toward the substrate is the complex nature of the solvent, composed of water and 2-propanol. The latter can undergo oxidative dehydrogenation to acetone which itself could adsorb on the surface preventing access of the substrate. The molar ratio between the substrate and 2-propanol in the current work varied in the range 0.02–0.2. Thus at high excess of the solvent (low substrate concentration) influence of it would be more prominent as the reaction proceeds since formed acetone can block the catalyst surface. Evaluation of the apparent reaction orders was done (Fig. 3) for the initial reaction rates, which minimizes the influence of 2-propanol oxidative dehydrogenation.

When the influence of oxygen partial pressure was studied (Fig. 4), the reaction rate was found to be independent on the oxygen amount following, thus, zero-order behavior.

The role of oxygen in selective oxidation reactions over gold catalysts was studied in a number of papers, where activated by the catalyst oxygen was found to: (a) interact with water, forming oxidizing active species [19,20]; (b) act as a Brønsted basic

site, enhancing O–H bond cleavage [21] as well as β-H removal which resulted in formation of corresponding aldehydes/ketones [17]; (c) scavenge the electrons deposited on gold during the reaction [22]. In the later work, the reaction rate of ethanol oxidation is increasing up to oxygen concentration of 10 vol.%, thereafter remaining constant. β-H removal is considered to be the limiting step of the oxidative dehydrogenation. However, this observation is not directly in line with HMR oxidation, where the reaction rate is independent on oxygen concentration in the domain studied (5–49 vol.%). At the same time, as was shown before [2] and mechanistically discussed in [13], in anaerobic conditions the reaction rate is dramatically decreased.

The reaction mechanism for aerobic oxidation of HMR can be considered to be similar to the one proposed for alcohols oxidation over gold [5,23] and described by Scheme 4.

HMR molecule can in principle be adsorbed on the catalyst surface due to interactions with positively charged sites of Au particles and/or Lewis acid sites of the support (Al) [24], and/or isolated OH-groups on the alumina surface [25], while α-H is removed by adsorbed oxygen acting as Brønsted basic sites. The formed intermediate undergoes β-H removal by the same Brønsted basic site, followed by oxoMAT formation.

Positively charged gold species were not detected by XPS in the previous work, moreover such adsorption would result in competition between HMR and adsorbed oxygen, therefore interactions with the Lewis sites and OH groups of the support are more probable as discussed in [14]. The cartoon on Scheme 4 explicitly illustrates that oxygen is adsorbed on sites different from HMR in line with the theoretical calculations in [13], data on the support influence [14] and kinetic data of the current study.

The reaction was performed over different amounts of the same catalyst (2 wt.% Au/Al₂O₃). The obtained HMR concentration

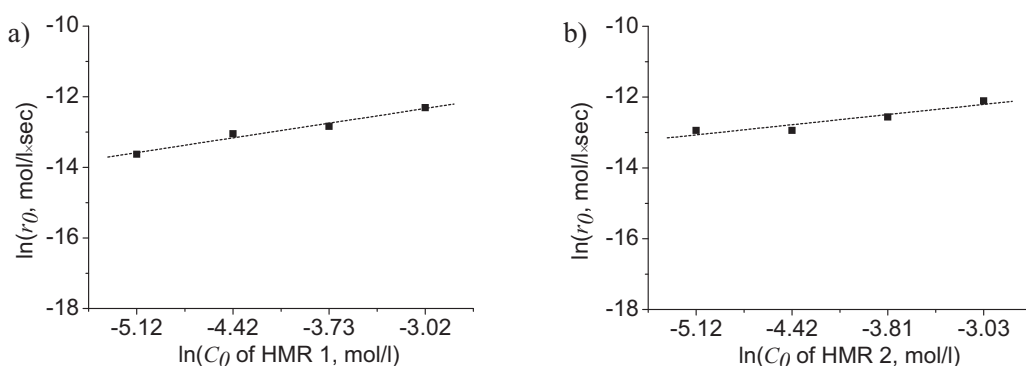


Fig. 3. Logarithm of initial reaction rate (r_0) of: (a) HMR 1 and (b) HMR 2 as a function of corresponding isomers initial concentration (C_0) logarithm.

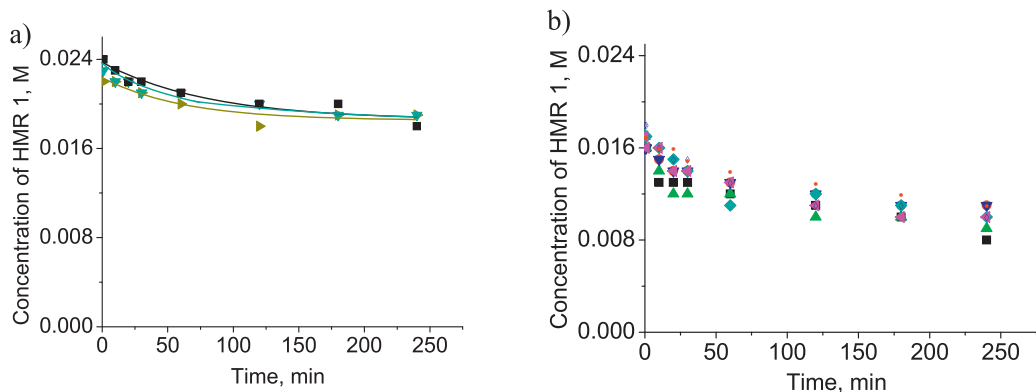
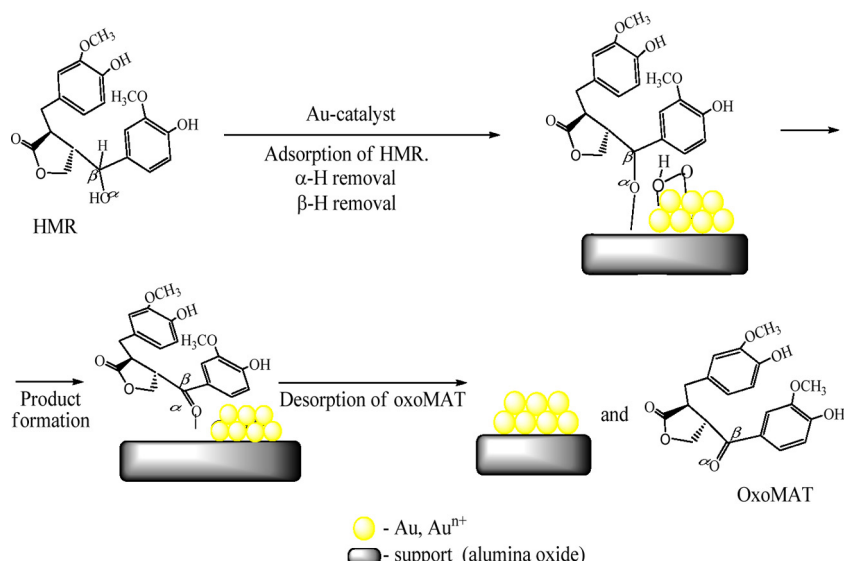


Fig. 4. Concentration vs. time dependence of: (a) HMR 1 and (b) HMR 2 over 250 mg 2 wt.% Au/Al₂O₃ catalyst at 70 °C, under different oxygen partial pressure: (●) 5.5%; (○) 8.6%; (▲) 12%; (◆) 24%; (▼) 32%; (■) 39%; (◀) 44%; (●) 49%.



Scheme 4. The proposed mechanism of HMR selective oxidation over supported gold catalyst.

profile versus time dependence is presented in Fig. 5. Calculations from the slope of the plot in logarithmic coordinates gave the first-order dependence with respect to the catalyst concentration (0.80 ± 0.08). This value was expected, while the slight deviation might be related to the catalyst deactivation demonstrated in [15].

3.1.2. Energy of activation of HMR oxidation/dehydrogenation

Fig. 6 shows the HMR concentration profiles during the reaction obtained at different temperatures. The apparent activation energy was calculated using the Arrhenius equation: $\ln k = -E/RT + \ln A$, where E – is the activation energy, R – is

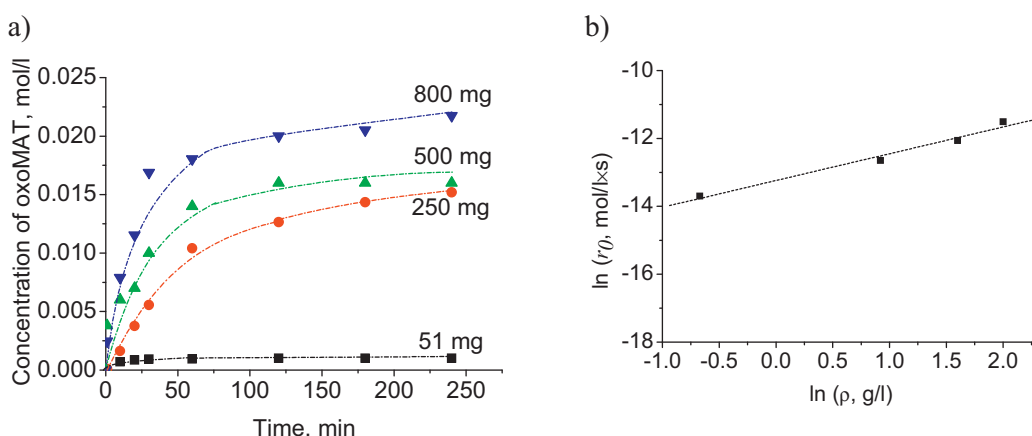


Fig. 5. (a) OxoMAT concentration profile at different catalyst mass loading and (b) linearization of the initial reaction rate (r_0 , mol/l/s) dependence on the catalyst loading (ρ , g/l).

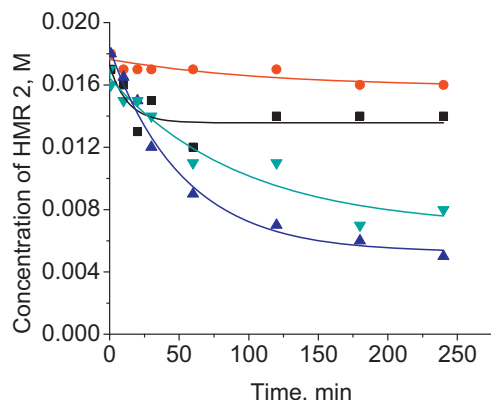


Fig. 6. Dependence of HMR 2 concentration on time over 200 mg of 2 wt.% Au/Al₂O₃ catalyst under 24% oxygen in nitrogen flow at different temperature: (●) at 30 °C; (■) at 50 °C; (▼) at 70 °C; (▲) at 90 °C.

the molar gas constant; T – temperature, A – pre-exponential factor.

Thus, apparent energy of activation calculated from the slope of the Arrhenius plot (Fig. 7) was found to be 43 ± 4.3 kJ/mol for HMR oxidation. For comparison, the apparent energy of activation of methanol [18] and ethanol [17] oxidation reactions over gold reported previously was 54 kJ/mol and 35 kJ/mol, respectively.

3.2. Kinetic modeling results

Reaction parameters were found from kinetic modeling and are listed in Table 1.

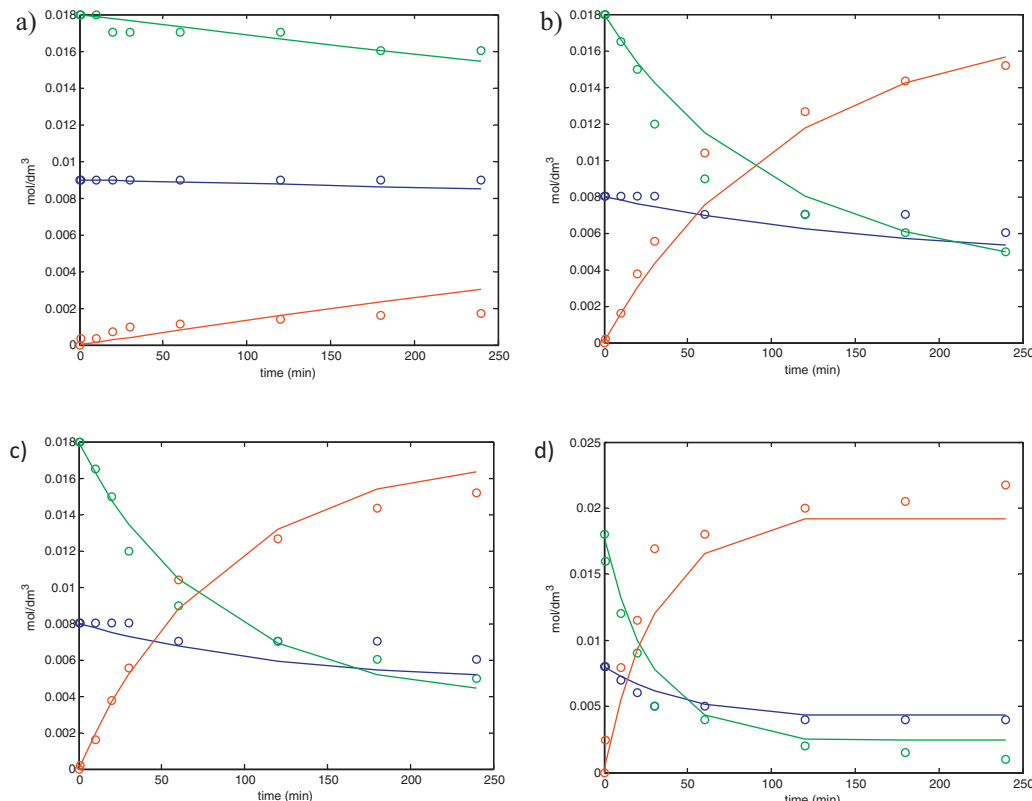


Fig. 8. Dependence of HMR 1 (blue), HMR 2 (green), oxoMAT (red) concentrations on time. Comparison of estimated curves (solid line) with experimental data (open circles). Oxidative dehydrogenation of HMR mixture under 22 vol.% oxygen in nitrogen over 2 wt.% Au/Al₂O₃ at: (a) 30 °C, catalyst mass 200 mg; (b) 70 °C, catalyst mass 200 mg; (c) 70 °C, catalyst mass 250 mg; and (d) 70 °C, catalyst mass 800 mg. (For interpretation of the references to color in this figure legend, the reader is referred to the web version of this article.)

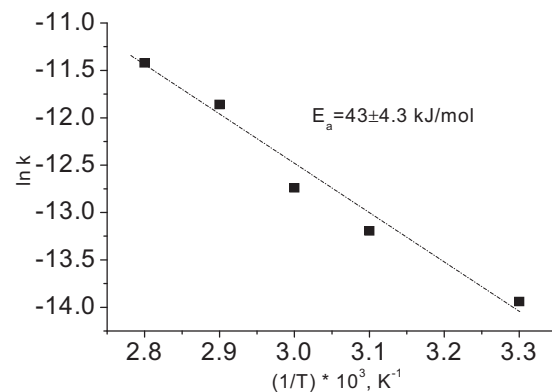


Fig. 7. Arrhenius plot of rate constant (k , s⁻¹) of HMR oxidation. Reaction conditions: HMR initial concentration 0.025 M, solvent 2 vol.% propan-2-ol in water, catalyst 200 mg, 24% oxygen in nitrogen flow.

Table 1

Results from parameter estimation of the HMR selective oxidation/dehydrogenation over gold catalysts (2 wt.% Au/Al₂O₃).

Parameter	HMR as a mixture of diastereomers	Isolated isomers (HMR 1 and HMR 2)
A_4 (min ⁻¹)	$(0.393 \pm 0.161) \times 10^{-2}$	$(0.165 \pm 0.005) \times 10^{-2}$
A_5 (min ⁻¹)	$(0.126 \pm 0.049) \times 10^{-1}$	$(0.426 \pm 0.016) \times 10^{-2}$
A_7 (min ⁻¹)	$(0.444 \pm 0.153) \times 10^{-3}$	$(0.144 \pm 0.008) \times 10^{-2}$
E_{a4} (kJ/mol)	$(0.500 \pm 0.153) \times 10^5$	
E_{a5} (kJ/mol)	$(0.543 \pm 0.039) \times 10^5$	
E_{a7} (kJ/mol)	$(0.853 \pm 0.163) \times 10^5$	
K_1 (dm ³ /mol)	$(0.865 \pm 0.351) \times 10^2$	7.58 ± 0.148
K_2 (dm ³ /mol)	$(0.763 \pm 0.712) \times 10^2$	32.4 ± 2.5
K_6^{-1} (dm ³ /mol)	$(0.135 \pm 0.107) \times 10^3$	0.368 ± 0.008

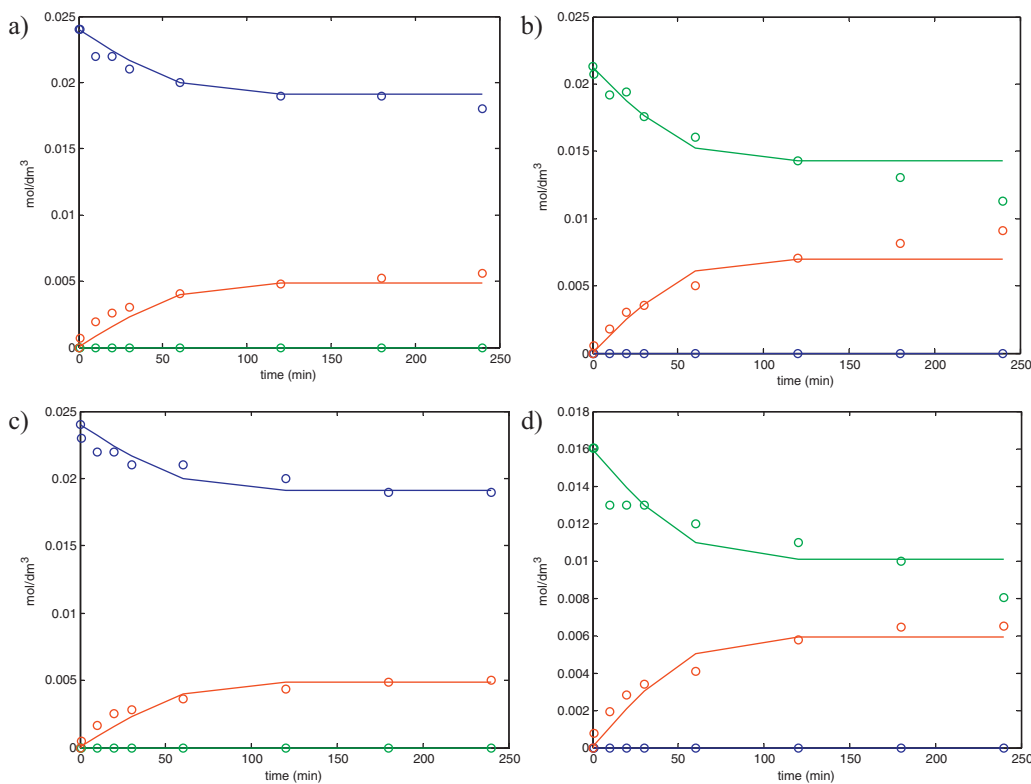


Fig. 9. Dependence of HMR 1 (blue), HMR 2 (green), oxoMAT (red) concentrations on time. Comparison of estimated curves (solid line) with experimental data (open circles). Oxidative dehydrogenation of isolated HMR 1 and HMR 2 over 2 wt.% Au/Al₂O₃: (a) at 70 °C, under 22 vol.% oxygen in nitrogen, catalyst mass 250 mg; (b) at 70 °C, under 22 vol.% oxygen in nitrogen, catalyst mass 250 mg; (c) at 70 °C, under 32 vol.% oxygen in nitrogen, catalyst mass 250 mg; and (d) at 70 °C, under 39 vol.% oxygen in nitrogen, catalyst mass 250 mg. (For interpretation of the references to color in this figure legend, the reader is referred to the web version of this article.)

The degree of explanation was 99.1% for the HMR isolated isomers and 92.4% for their mixtures. The simulated curves were compared with the experimental data and presented in Fig. 8.

The model corresponds better with experiments in the case of isolated isomers transformation, while the simulation of the reaction using diastereomers mixtures as a starting material has shown some underestimation (Fig. 9). The observed difference in the reaction rate between transformation of HMR utilized as a mixture of isomers and isolated ones can be tentatively explained by competitive adsorption of isomers on the catalyst surface or presence of impurities, which can have a detrimental effect on the catalyst performance [15].

4. Conclusions

The kinetic regularities of the gold catalyzed aerobic selective oxidation of a naturally occurring lignin hydroxymatairesinol (HMR) were revealed. The reaction was found to be zero-order with respect to oxygen, being the first-order with respect to the catalyst. The reaction order toward HMR isomers was fractional. The retardation of the reaction rate with the product formation was attributed to the strong adsorption of oxoMAT on the gold surface as well as deactivation. The values of the rate and adsorption constants were estimated through numerical data fitting.

Acknowledgements

The authors express their gratitude to Dr. Lari Vähäsalo for HMR preparation, Mr. Jarl Hemming and Mr. Markku Reunanan for product identification.

References

- [1] S. Willför, J. Hemming, M. Reunanan, C. Eckerman, B. Holmbom, *Holzforschung* 57 (2003) 27–36.
- [2] O.A. Simakova, E.V. Murzina, P. Mäki-Arvela, A.-R. Leino, B.C. Campo, K. Kordas, S. Willför, T. Salmi, D.Y. Murzin, *J. Catal.* 282 (2011) 54–64.
- [3] H. Korte, M. Unkila, M. Hiirola-Taijö, V.-M. Lehtola, M. Ahotupa, Patent WO/2004/000304 A1 (2003).
- [4] T. Ahlnäs, Patent WO 2008/020112 A1 (2008).
- [5] A. Abad, C. Almela, A. Corma, H. Garcia, *Tetrahedron* 62 (2006) 6666–6672.
- [6] H. Li, B. Guan, W. Wang, D. Xing, Z. Fang, X. Wan, L. Yang, Z. Shi, *Tetrahedron* 63 (2007) 8430–8434.
- [7] L.-C. Wang, L. He, Q. Liu, Y.-M. Liu, M. Chen, Y. Cao, H.-Y. He, K.-N. Fan, *Appl. Catal. A* 344 (1–2) (2008) 150–157.
- [8] X. Wang, H. Kawanami, S.E. Dapurkar, N.S. Venkataraman, M. Chatterjee, T. Yokoyama, Y. Ikushima, *Appl. Catal. A* 349 (2008) 86–90.
- [9] M. Kidwai, S. Bhardwaj, *Appl. Catal. A* 387 (2010) 1–4.
- [10] S. Ivanova, V. Pitchon, Y. Zimmermann, C. Petit, *Appl. Catal. A* 298 (2006) 57–64.
- [11] H. Markus, P. Mäki-Arvela, N. Kumar, N.V. Kul'kova, P. Eklund, R. Sjöholm, B. Holmbom, T. Salmi, D.Y. Murzin, *Catal. Lett.* 103 (2005) 125–131.
- [12] H. Haario, MODEST 6.0 – User's Guide, Profmath Oy, Helsinki, 2001.
- [13] A. Prestianni, F. Ferrante, O.A. Simakova, D. Duca, D.Y. Murzin, *Chem. Eur. J.* 19 (2013) 4577–4585.
- [14] O. Simakova, E. Smolentseva, M. Estrada, E. Murzina, S. Beloshapkin, S. Willför, A. Simakov, D.Y. Murzin, *J. Catal.* 291 (2012) 95–103.
- [15] O.A. Simakova, E.V. Murzina, A.-R. Leino, P. Mäki-Arvela, S.M. Willför, D.Y. Murzin, *Catal. Lett.* 142 (2012) 1011–1019.
- [16] B. Jørgensen, S. Egholm Christiansen, M.L. Dahl Thomsen, C.H. Christensen, *J. Catal.* 251 (2007) 332–337.
- [17] Y. Guan, E.J.M. Hensen, *Appl. Catal. A* 361 (2009) 49–56.
- [18] Q. Deng, X. Li, Z. Peng, Y. Long, L. Xiang, T. Cai, *Trans. Nonferrous Met. Soc. China* 20 (2010) 437–442.
- [19] X. Yang, X. Wang, C. Liang, W. Su, C. Wang, Z. Feng, C. Li, J. Qiu, *Catal. Commun.* 9 (2008) 2278–2281.
- [20] B.N. Zope, D.D. Hibbitts, M. Neurock, R.J. Davis, *Science* 330 (2010) 74–78.
- [21] B.K. Min, C.M. Friend, *Chem. Rev.* 107 (2007) 2709–2724.
- [22] S.E. Davis, B.N. Zope, R.J. Davis, *Green Chem.* 14 (2012) 143–147.
- [23] M. Boronat, A. Corma, F. Illas, J. Radilla, T. Rodenas, M. Sabater, *J. Catal.* 278 (2011) 50–58.
- [24] S. Cai, K. Sohlberg, *J. Mol. Catal. A* 193 (2003) 157–164.
- [25] Z. Martinez-Ramirez, S.A. Jimenez-Lam, L.C. Fierro-Gonzalez, *J. Mol. Catal. A* 344 (2011) 47–52.